WALAILAK JOURNAL
http://wjst.wu.ac.th Engineering and Physical Sciences

Heat Transfer for MHD Second Grade Fluid Flow over a Porous Nonlinear Radially Stretching Sheet

Asif MUNIR[1,*], Azeem SHAHZAD[2] and Masood KHAN[1]

[1]*Department of Mathematics, Quaid-i-Azam University, Islamabad, Pakistan*
[2]*Department of Basic Science, University of Engineering & Technology, Taxila, Pakistan*

([*]Corresponding author's e-mail: asifmunir1000@yahoo.com)

Received: 8 December 2013, Revised: 14 May 2014, Accepted: 26 June 2014

Abstract

The heat transfer for the steady axisymmetric flow of a second grade fluid over an isothermal radially stretching porous sheet is investigated. A power law stretching of sheet is assumed, while the fluid is electrically conducting in the presence of a transverse magnetic field. Appropriate similarity transformations are introduced to reduce the resulting highly non-linear partial differential equations into ordinary differential equations, which are then solved analytically by the homotopy analysis method (HAM) and numerically by the shooting method using the adaptive Runge Kutta method with Broyden's method. The developed analytical expressions for the temperature field are graphically presented and the influence of pertinent parameters on the thermal boundary layer is discussed in detail. To check the reliability of the HAM results, a comparison is made with numerical results. An excellent agreement is observed between the 2 sets of results. In addition, the local Nusselt number is tabulated for several influential parameters.

Keywords: Heat transfer, second grade fluid, radially stretching sheet

Introduction

Recently, many efforts have been made to investigate the boundary layer flows on heated continuous stretching surfaces, owing to their tremendous applications in industries. These applications include paper production, materials manufactured by the extrusion process, production of polymer films, the boundary layer along a liquid film in the condensation process, and the heat treated materials traveling between a feed roll and the wind-up roll or on a conveyor belt which poses the features of a moving continuous surface. The final product with the desired characteristics strictly depends upon the stretching rate and the rate of cooling in the process. Carragher *et al.* [1] investigated the heat transfer of the viscous fluid over stretching surface under the conditions when the temperature difference between the surface and the ambient fluid is proportional to a power of distance from a fixed point. Cortel [2] considered the flow and heat transfer of a viscous fluid over nonlinear stretching sheet. Recently, Alinejad and Samarbakhsh [3] examined the effects of viscous dissipation on viscous flow over nonlinear stretching sheet.

The non-Newtonian fluids are nowadays acknowledged as more suitable for scientific and technological applications than Newtonian fluids [4]. Numerous materials, such as salt and polymer solutions or melts, drilling mud, starch suspensions, cements, certain oils and greases, and many emulsions, are classified as non-Newtonian fluids. Due to the vast potential for research in industrial applications, researchers are analyzing the flow and heat transfer characteristics of such fluids. One can refer to the recent work of Liu [5] who gave analytical solutions for the steady boundary layer flow and heat transfer of an electrically conducting second grade fluid past a semi-infinite stretching sheet. Singh and Agarwal [6] analyzed the boundary layer flow and heat transfer characteristics of a second grade fluid over an exponentially stretching sheet. Hayat *et al*. [7] analyzed the flow and heat transfer of a second grade fluid

with convective boundary condition. Hayat *et al*. [8] also investigated the Newtonian heating effects in boundary layer flow of a second grade fluid over a stretching sheet.

A vast amount of literature is now available regarding the laminar boundary layer flow and heat transfer of viscous and differential type fluids over a planner stretching sheet. However, a relatively scarce amount of information regarding the flow and heat transfer over a radially stretching sheet is observed in literature. The work of Arial [4] can be cited, who studied the axisymmetric flow of a second grade fluid over radially stretching sheet, and derived perturbation and asymtotic solutions for small and large values of the viscoelastic parameter, respectively. Hayat and Sajid [9] extended the work of Arial [4] and examined the heat transfer for the flow of a second grade fluid over radially stretching sheet, and found analytic solutions using the homotopy analysis method. Sahoo [10] examined the effects of slip, viscous dissipation, and Joule heating on the magneto hydrodynamic flow and heat transfer of a second grade fluid over a radially stretching sheet. Ahmad *et al.* [11] considered the heat transfer characteristics due to unsteady axisymmetric flow of a second grade fluid. All of the above studies are limited to flow and heat transfer over linear radially stretching sheets. However, as pointed out by Gupta and Gupta [12], realistically, stretching of the sheet may not necessarily be linear. This situation was dealt by Shahzad *et al*. [13] in their work on the exact solution for axisymmetric flow and heat transfer over a nonlinear radially stretching sheet. They considered viscous fluid and assumed the stretching velocity in the form $U(r) = cr^3$.

In the present investigation we consider the heat transfer due to flow of a second grade fluid and assume the stretching velocity in the form $U(r) = cr^n$, where n is a positive real number and c is a positive constant. The boundary layer equations are derived by using boundary layer approximations, and the modelled non-linear coupled partial differential equations are reduced to 2 point boundary value problems, using proper similarity transformations. The homotopy analysis method (HAM) and shooting method, using the adaptive Runge Kutta method with Broyden's method, are employed for solutions.

Mathematical formulation

Consider the quiescent and electrically conducting second grade fluid in the presence of a transverse magnetic field. A steady, laminar, and axisymmetric flow is induced, due to a stretching of the sheet along the radial direction, with power law velocity given by $U_w = cr^n$. We assume that the sheet is isothermal with temperature T_w while T_∞ is the ambient fluid temperature with $T_w > T_\infty$. The magnetic field $\mathbf{B} = [0, 0, B_0]$ is applied perpendicular to the sheet, as shown in **Figure 1**. Magnetic Reynolds number is assumed to be vanishingly small, so that the induced magnetic field is neglected in comparison with the applied magnetic field.

The constitutive equation of an incompressible homogeneous second grade fluid is [14];

$$\mathbf{T} = -p\mathbf{I} + \mu\mathbf{A}_1 + \alpha_1\mathbf{A}_2 + \alpha_2\mathbf{A}_1^2, \tag{1}$$

where $\mathbf{T}$ is the Cauchy stress tensor. p is the pressure. μ is the dynamic viscosity. α_1, α_2 are material parameters. $\mathbf{A}_1$ and $\mathbf{A}_2$ the first 2 Rivlin-Ericksen tensors, given by;

$$\begin{aligned} \mathbf{A}_1 &= (\operatorname{grad}\mathbf{v}) + (\operatorname{grad}\mathbf{v})^T, \\ \mathbf{A}_2 &= \frac{d\mathbf{A}_1}{dt} + \mathbf{A}_1(\operatorname{grad}\mathbf{v}) + (\operatorname{grad}\mathbf{v})^T\mathbf{A}_1, \end{aligned} \tag{2}$$

where $\mathbf{v}$ denotes the velocity field and $\frac{d}{dt}$ is the material derivative.

The Clausius-Duhem inequality and the minimum Helmholtz free energy in equilibrium require that $\mu \geqslant 0,\ \alpha_1 \geqslant 0, \alpha_1 + \alpha_2 = 0$.

The flow is 2-dimensional and bidirectional and velocity field is of the form;

$$\mathbf{v} = [u(r,z), 0, w(r,z)]. \tag{3}$$

Under the above velocity field, the continuity equation and momentum equation for steady flow are written as;

$$\frac{\partial u}{\partial r} + \frac{u}{r} + \frac{\partial w}{\partial z} = 0, \tag{4}$$

$$\rho\left(u\frac{\partial u}{\partial r} + w\frac{\partial u}{\partial z}\right) = \frac{\partial T_{rr}}{\partial r} + \frac{\partial T_{rz}}{\partial z} + \frac{T_{rr} - T_{\theta\theta}}{r} - \sigma B_0 u, \tag{5}$$

$$\rho\left(u\frac{\partial w}{\partial r} + w\frac{\partial w}{\partial z}\right) = \frac{1}{r}\frac{\partial}{\partial r}(rT_{rz}) + \frac{\partial T_{zz}}{\partial z}, \tag{6}$$

where σ is the electrical conductivity and ρ is the density.

The non-vanishing components of stress tensor $\mathbf{T}$ are T_{rr}, $T_{\theta\theta}$, T_{zz} and T_{rz} and given by;

$$T_{rr} = -p + 2\mu\frac{\partial u}{\partial r} + 2\alpha_1\left[u\frac{\partial^2 u}{\partial r^2} + w\frac{\partial^2 u}{\partial r\partial z} + 2\left(\frac{\partial u}{\partial r}\right)^2 + \frac{\partial w}{\partial r}\left(\frac{\partial u}{\partial z} + \frac{\partial w}{\partial r}\right)\right], \\ +\alpha_2\left[4\left(\frac{\partial u}{\partial r}\right)^2 + \left(\frac{\partial u}{\partial z} + \frac{\partial w}{\partial r}\right)^2\right], \tag{7}$$

$$T_{\theta\theta} = -p + 2\mu\frac{u}{r} + 2\alpha_1\left(\frac{u}{r}\frac{\partial u}{\partial r} + \frac{w}{r}\frac{\partial u}{\partial z} + \frac{u^2}{r^2}\right) + 4\alpha_2\frac{u^2}{r^2}, \tag{8}$$

$$T_{zz} = -p + 2\mu\frac{\partial w}{\partial z} + 2\alpha_1\left[u\frac{\partial^2 w}{\partial r\partial z} + w\frac{\partial^2 w}{\partial z^2} + 2\left(\frac{\partial w}{\partial z}\right)^2 + \frac{\partial u}{\partial z}\left(\frac{\partial u}{\partial z} + \frac{\partial w}{\partial r}\right)\right] \\ +\alpha_2\left[4\left(\frac{\partial w}{\partial z}\right)^2 + \left(\frac{\partial u}{\partial z} + \frac{\partial w}{\partial r}\right)^2\right], \tag{9}$$

$$T_{rz} = \mu\left(\frac{\partial u}{\partial z} + \frac{\partial w}{\partial r}\right) + \alpha_1\left[\left(u\frac{\partial}{\partial r} + w\frac{\partial}{\partial z}\right)\left(\frac{\partial u}{\partial z} + \frac{\partial w}{\partial r}\right) + \frac{\partial u}{\partial r}\frac{\partial w}{\partial r} + \frac{\partial u}{\partial z}\frac{\partial w}{\partial z}\right. \\ \left. +3\left(\frac{\partial u}{\partial r}\frac{\partial u}{\partial z} + \frac{\partial w}{\partial r}\frac{\partial w}{\partial z}\right)\right] + 2\alpha_2\left(\frac{\partial u}{\partial r} + \frac{\partial w}{\partial z}\right)\left(\frac{\partial u}{\partial z} + \frac{\partial w}{\partial r}\right). \tag{10}$$

Applying the boundary layer approximation, we obtain the following governing equation;

$$u\frac{\partial u}{\partial r}+w\frac{\partial u}{\partial z}=\nu\frac{\partial^2 u}{\partial z^2}+\frac{\alpha_1}{\rho}\left(u\frac{\partial^3 u}{\partial r\partial z^2}+w\frac{\partial^3 u}{\partial z^3}+\frac{\partial u}{\partial r}\frac{\partial^2 u}{\partial z^2}+\frac{\partial u}{\partial z}\frac{\partial^2 u}{\partial r\partial z}\right)-\sigma\frac{B_0^2 u}{\rho}, \quad (11)$$

where ν is the kinematic viscosity. The corresponding velocity field boundary conditions are;

$$u=U(r)=cr^n, \;\; w=-V_w \quad at \quad z=0, \tag{12}$$

$$u\to 0 \quad as \quad z\to\infty, \tag{13}$$

where V_w is the porosity of the sheet.

We use the following similarity transformations;

$$\psi(r,z)=-r^2U\,\mathrm{Re}^{-\frac{1}{2}}f(\eta), \text{ and } \eta=\frac{z}{r}\mathrm{Re}^{\frac{1}{2}}, \tag{14}$$

where *h* is the dimensionless similarity variable. $\mathrm{Re}=\frac{Ur}{\nu}$ is the local Reynolds number. $\psi(r,z)$ is the Stokes stream function defined by $u=-\frac{1}{r}\frac{\partial\psi}{\partial z}$ and $w=\frac{1}{r}\frac{\partial\psi}{\partial r}$, giving;

$$u=Uf'(\eta) \text{ and } w=-U\,\mathrm{Re}^{-\frac{1}{2}}\left[\frac{n+3}{2}f(\eta)+\frac{n-1}{2}\eta f'(\eta)\right]. \tag{15}$$

After utilizing the above similarity transformations, Eqs. (11) to (13) reduce to;

$$f'''+\frac{n+3}{2}ff''-n\left(f'\right)^2+\alpha\left\{\left(3n-1\right)f'f''+\frac{3n-1}{2}\left(f''\right)^2 -\frac{n+3}{2}ff''''+(n-1)f''f'''\right\}-M^2f'=0, \tag{16}$$

$$f(0)=s, \;\; f'(0)=1 \text{ and } f'(\infty)=0, \tag{17}$$

where $\alpha=\frac{\alpha_1 U}{r\mu}$ is the dimensionless second grade parameter. $M=(\frac{sB_0^2r^{1-n}}{rc})^{1/2}$ is the local magnetic parameter. $s=\frac{2V_m}{(n+3)\sqrt{\nu c}}r^{(1-n)/2}$ is the local mass transfer parameter, with $s>0$ for mass suction and $s<0$ for mass injection.

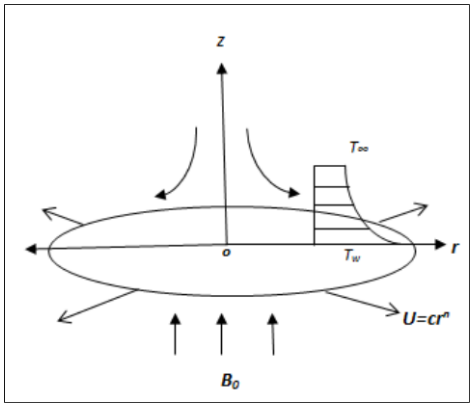


Figure 1 Configuration of the flow and geometrical coordinates.

Heat transfer problem

Ignoring the radiant heat transfer, and in the absence of viscous dissipation and heat generation, the energy equation for temperature field $T = T(r,z)$ is;

$$\rho c_p \left(u\frac{\partial T}{\partial r} + w\frac{\partial T}{\partial z} \right) = \kappa \left(\frac{\partial^2 T}{\partial r^2} + \frac{1}{r}\frac{\partial T}{\partial r} + \frac{\partial^2 T}{\partial z^2} \right), \tag{18}$$

where c_p is the specific heat at constant pressure and κ is the thermal conductivity.

The thermal boundary layer approximations reduce the above equation to;

$$u\frac{\partial T}{\partial r} + w\frac{\partial T}{\partial z} = \frac{\kappa}{\rho c_p}\frac{\partial^2 T}{\partial z^2}, \tag{19}$$

subject to the boundary conditions;

$$T = T_w \quad \text{at} \quad z = 0, \tag{20}$$

$$T = T_\infty \quad \text{as} \quad z \to \infty, \tag{21}$$

where T_w is the sheet temperature and T_∞ is the temperature of surrounding fluid.

Using the similarity variables (14) and;

$$\theta(\eta) = \frac{T - T_\infty}{T_w - T_\infty}, \tag{22}$$

Eqs. (19) to (21) take the form;

$$\theta'' + \Pr \frac{n+3}{2} f\theta' = 0, \tag{23}$$

$$\theta(0) = 1,\ \theta(\infty) = 0, \tag{24}$$

with $\Pr = \frac{mc_p}{k}$ as the Prandtl number.

The local Nusselt number (Nu_r) is defined as;

$$Nu_r = \frac{rq_w}{\kappa(T_w - T_\infty)}\bigg|_{z=0}, \tag{25}$$

where the wall heat flux q_w is given by;

$$q_w = -\kappa\left(\frac{\partial T}{\partial z}\right)\bigg|_{z=0}, \tag{26}$$

which by virtue of Eq. (22) reduces to;

$$\mathrm{Re}^{-1/2} Nu_r = -\theta'(0). \tag{27}$$

Solution of the problem

The homotopy analysis method (HAM) is an analytic approximation method to find the solution of highly nonlinear differential equations. In order to find the analytic solutions of Eqs. (16) and (23), subject to boundary conditions (17) and (24), by the homotopy analysis method (HAM), we choose the initial guesses $f_0(\eta)$ and $\theta_0(\eta)$ to the final solutions $f(\eta)$ and $\theta(\eta)$ as;

$$f_0(\eta) = s + 1 - \exp(-\eta),\ \theta_0(\eta) = \exp(-\eta), \tag{28}$$

and the auxiliary linear operators as;

$$\mathcal{L}_f(\phi) = \frac{d^3\phi}{d\eta^3} - \frac{d\phi}{d\eta},\ \mathcal{L}_\theta(\phi) = \frac{d^2\phi}{d\eta^2} - \frac{d\phi}{d\eta}. \tag{29}$$

Now, by letting $\hbar_f$ and $\hbar_\theta$ as the auxiliary convergence control parameters, we can construct the zero and higher order deformation problems in view of references [9,13]. The auxiliary parameters $\hbar_f$ and $\hbar_\theta$ adjust and control the convergence of the series solutions. The optimal values of these convergence control parameters are chosen by minimizing the discrete squared residual [15], given by;

$$E_{f,m} = \frac{1}{N+1}\sum_{j=0}^{N}\left[N_f\left(\sum_{i=0}^{m} F_j(i\triangle\eta)\right)\right]^2, \tag{30}$$

$$E_{\theta,m} = \frac{1}{N+1}\sum_{j=0}^{N}\left[N_\theta\left(\sum_{i=0}^{m} G_j(i\triangle\eta)\right)\right]^2. \quad (31)$$

where $N+1$ is the number of points, chosen over the domain in which the nonlinear equations $N_f(f(\eta)) = 0$ and $N_\theta(\theta(\eta)) = 0$ are defined. **Table 1** shows the convergence of series solution for optimum value of convergence control parameters h_q.

Table 1 The analytical approximation of $\theta'(0)$ when $s = 0.3$, $\alpha = 0.1$, $M = 1.0$, $n = 0.5$ and $\Pr = 0.7$ are fixed.

Order of approximation	h_θ = **–0.91054 (optimum)**
	$\theta'(0)$
5	-0.88687
10	-0.88086
15	-0.88023
20	-0.88020
21	-0.88020
22	-0.88020

Table 2 The values of local Nu_r when $M = 0.5$.

Pr	s	n	α	$-\theta'(0)$ (HAM results)	$-\theta'(0)$ (Numerical results)
0.3	0.5	2.0	0.5	0.74849	0.74849
0.3	0.5	2.0	0.5	1.13366	1.13365
0.7	0.5	2.0	0.5	1.48515	1.48515
0.7	0.5	0.5	0.5	1.10818	1.10817
0.7	0.5	1.0	0.5	1.23748	1.23749
0.7	0.5	2.0	0.5	1.48516	1.48515
0.7	0.1	2.0	0.5	0.94811	0.94811
0.7	0.2	2.0	0.5	1.07567	1.07566
0.7	-0.1	2.0	0.5	0.71050	0.71050
0.7	-0.2	2.0	0.5	0.60196	0.60194
0.7	0.5	2.0	0.0	1.31656	1.31656
0.7	0.5	2.0	0.2	1.42463	1.42462
0.7	0.5	2.0	0.5	1.48517	1.48515

Results and discussion

The resulting boundary value problem given by Eqs. (16) and (23) are solved for isothermal sheet. Solutions are obtained analytically, using the HAM and numerically by the shooting method using the adaptive Runge Kutta method with Broyden's method. The effects of n, Pr, s, α and M on temperature field are shown graphically. Moreover, the variation of local Nusselt with suction/injection for different Prandtl numbers and second grade parameters is also presented with graphs. Numerical values of the local Nusselt number by varying different pertinent parameters are also tabulated. The comparison of analytical and numerical values obtained from the HAM and shooting method is also given in this table.

Stretching parameter n affects the thermal boundary layer markedly. **Figure 2a** depicts the temperature profile for different values of stretching parameter n. This figure shows that the thermal boundary layer decreases with the increasing value of the stretching parameter. Pr has a significant role in controlling the thermal boundary layer thickness. The effects of Pr on the thermal boundary layer for fixed values of other parameters are illustrated in **Figure 2b**. It depicts that the effect of Pr on thermal boundary layer is very prominent. It is noted that an increase in Pr decreases the thermal boundary layer thickness, which results in augmentation of heat transfer at the wall.

The effects of suction on thermal boundary layer thickness are presented in **Figure 3**. This **Figure 3a** elucidates that the thermal boundary layer decreases due to suction of fluid near the sheet. The suction improves the heat transfer coefficient. The effects of injection on thermal boundary layer thickness are illustrated in **Figure 3b**. Here, we can see that the injection increases the fluid temperature and thermal boundary layer, due to a decrease in heat transfer coefficient.

The effects of α and M on temperature profile are elucidated in **Figure 4**. The detailed examination of **Figure 4a** shows the progressive thinning of the thermal boundary layer with the increasing α, irrespective of the values of the other parameters. This in turn enhances the heat transfer at the wall. This figure also compares the thermal boundary layer thickness between Newtonian and second grade fluids, and indicates that the thermal boundary layer for a Newtonian fluid is larger as compared to that of second grade fluid. **Figure 4b** illustrates the effect of magnetic parameter M. The effects of M on the thermal boundary layer are not very prominent; however, the temperature profile increases by increasing M.

The effects of suction and injection on local Nu_r are shown in **Figure 5**. **Figure 5a** depicts that increasing suction parameter increases the local Nu_r. Moreover, this figure also shows that Nu_r enhances with increase in Pr. This figure further illustrates that augmentation of the second grade parameter α boosts the heat transfer at the wall for the same value of Pr. Finally, for comparison, the profiles of temperature are sketched in **Figures 6a** and **6b**. Solid lines are the HAM solutions, while open circles are numerical solutions. This comparison shows a very good agreement between both the solutions. The agreement between the HAM and the numerical results confirm the accuracy of the analytical results.

Table 2 gives the variation of the local Nu_r by changing parameters, like Pr, s and a, keeping other parameters fixed. From this table, it is noted that the local Nu_r increases when Pr, a, n, and suction are increased. On the other side, an increase in injection decreases the local Nu_r.

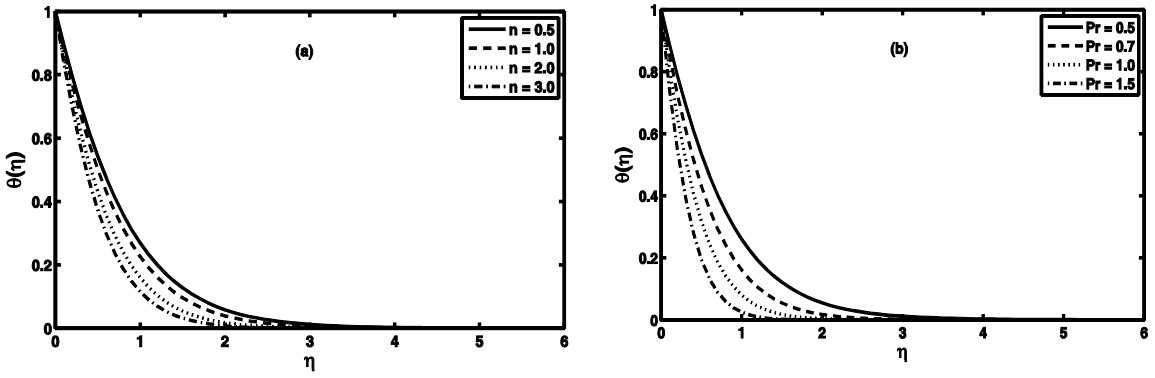


Figure 2 Influence of the n and Pr on temperature $\theta(\eta)$ when $n = 2$, $\alpha = 0.5$, $M = 1$ and $s = 0.5$ are fixed.

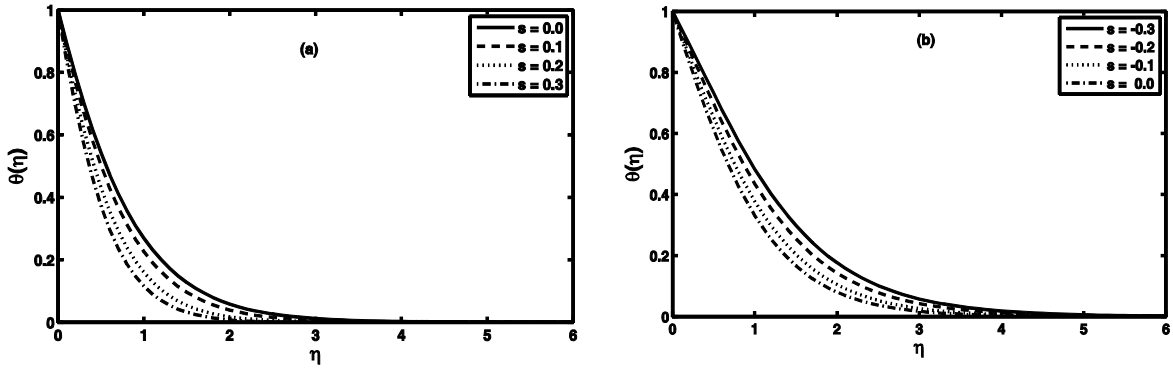


Figure 3 Influence of the s on temperature $\theta(\eta)$ when $n = 2, M = 1, \alpha = 0.5$ and $\Pr = 0.7$ are fixed.

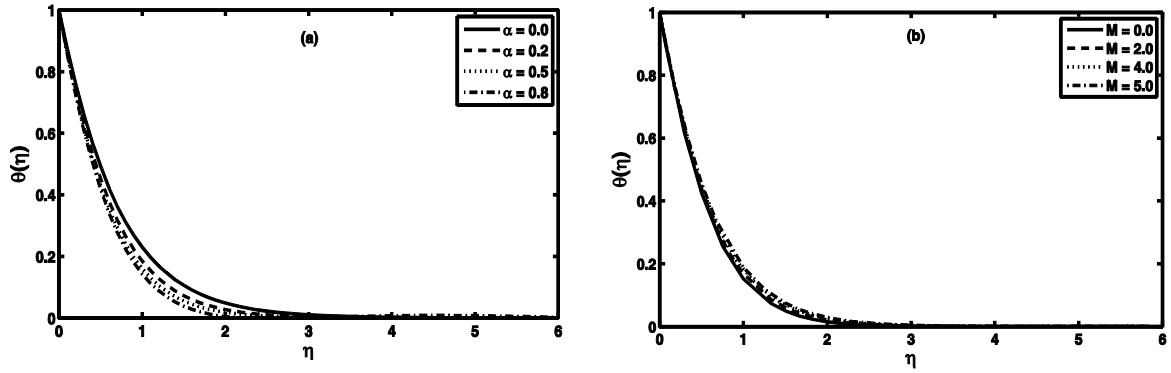


Figure 4 Influence of the α and M on temperature $\theta(\eta)$ when $n = 2$, $\Pr = 0.7$ and $s = 0.5$ are fixed.

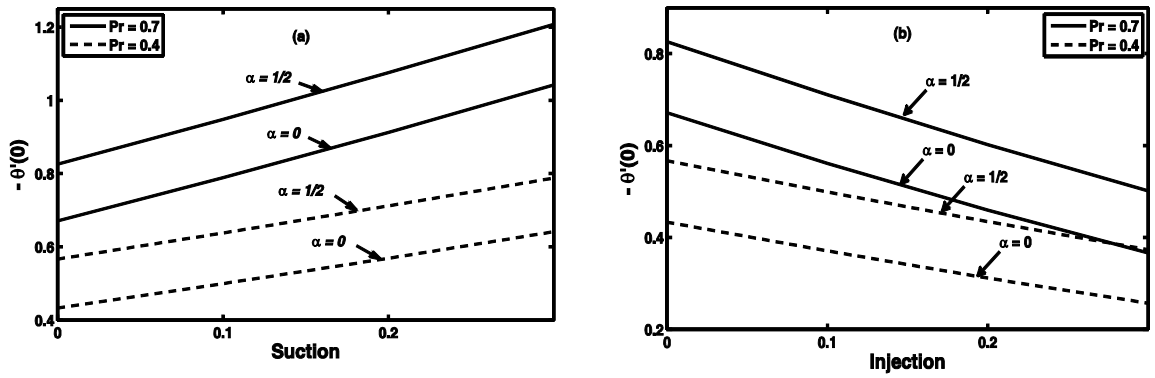


Figure 5 Influence of the local mass transfer parameters on local Nu_r for $\alpha = 0$ and $\alpha = 0.5$ when $n = 2$, $M = 1$ are fixed.

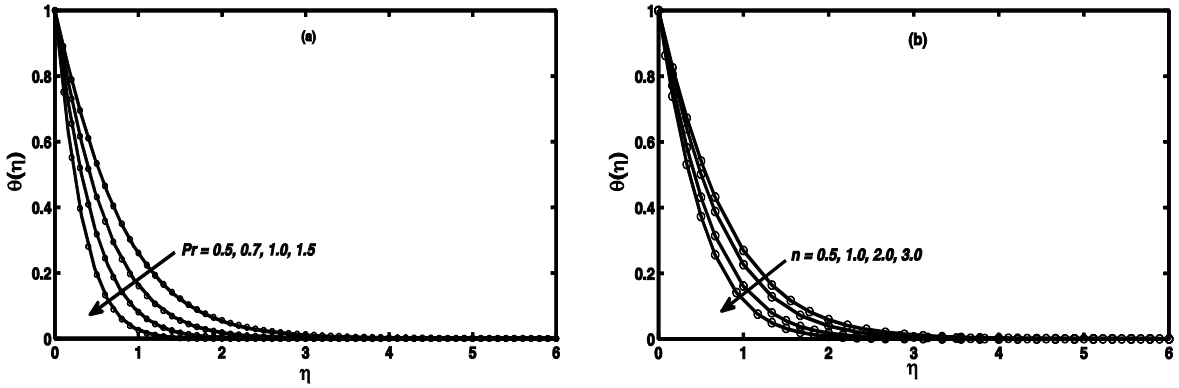


Figure 6 A comparison of the HAM and numerical results (solid line HAM result and open circles numerical results).

Conclusions

In this article, the HAM was applied to analyze the heat transfer due to an axisymmetric flow of an electrically conducting second grade fluid over a non-linear radially stretching porous sheet. The analytical solutions were obtained and verified by numerical results. The following conclusions were drawn from this study:

1) An increase in Pr, n, α and suction reduced the thermal boundary layer thickness and increased the local Nusselt number.

2) The Pr affected the thermal boundary layer more strongly as compared to other physical parameters.

3) An increase in injection increased the thermal boundary layer thickness and decreased the local Nu_r.

4) The local Nu_r increased by an increase in suction. This increase was sharper than that for larger.

5) The decrease in local Nu_r was noticed with an increase in injection. This decrease was sharper than that for smaller Pr.

6) There was a boost in the local Nu_r with an increase in a.

Acknowledgment

This work has the financial support of the Higher Education Commission (HEC) of Pakistan.

References

[1] P Carragher and LJ Crane. Heat transfer on a continuous stretching sheet. *Z. Angew. Math. Mech.* 1982; **62**, 564-73.
[2] R Cortell. Viscous flow and heat transfer over a nonlinearly stretching sheet. *Appl. Math. Comput.* 2007; **184**, 864-73.
[3] J Alinejad and S Samarbakhsh. Viscous flow over nonlinearly stretching sheet with effects of viscous dissipation. *J. Appl. Math.* 2012; **2012**, 587834.
[4] PD Ariel. A numerical algorithm for computing the stagnation point flow of a second grade fluid with/without suction. *J. Comput. Appl. Math.* 1995; **59**, 9-24.
[5] C Liu. Flow and heat transfer of an electrically conducting fluid of second grade in a porous medium over a stretching sheet subject to a transverse magnetic field. *Int. J. Heat Mass Tran.* 2004; **47**, 4427-37.
[6] V Singh and S Agarwal. Heat transfer in a second grade fluid over an exponentially stretching sheet through porous medium with thermal radiation and ellastic deformation under the effects of magnetic field. *Int. J. Appl. Math. Mech.* 2012; **8**, 41-63.
[7] T Hayat, SA Shehzad, M Qasim and S Obaidat. Flow of a second grade fluid with convective boundary conditions. *Therm. Sci.* 2011; **15**, 253-61.
[8] T Hayat, Z Iqbal and M Mustafa. Flow of a second grade fluid over a stretching surface with Newtonian heating. *J. Mech.* 2012; **28**, 209-16.
[9] T Hayat and M Sajid. Analytic solution for axisymmetric flow and heat transfer of second grade fluid past a stretching sheet. *Int. J. Heat Mass Tran.* 2007; **50**, 75-84.
[10] B Sahoo. Effects of slip, viscous dissipation and Joule heating on the MHD flow and heat transfer of a second grade fluid past a radially stretching sheet. *Appl. Math. Mech.* 2010; **31**, 159-73.
[11] I Ahmad, M Sajid and T Hayat. Heat transfer in unsteady axisymmetric second grade fluid. *Appl. Math. Comput.* 2009; **215**, 1685-95.
[12] PS Gupta and AS Gupta. Heat and mass transfer on a stretching sheet with suction or blowing. *Can. J. Chem. Eng.* 1977; **55**, 744-6.
[13] A Shahzad, R Ali and M Khan. On the exact solution for axisymetric flow and heat transfer over a nonlinear radially stretching sheet. *Chin. Phys. Lett.* 2012; **29**, 084705.
[14] RS Rivlin and JL Ericksen. Stress deformation relations for isotropic materials. *J. Rat. Mech. Anal.* 1955; **4**, 323-425.
[15] S Liao. *Homotopy Analysis Method in Nonlinear Differential Equations*. Springer, New York, 2012, p. 1-119.